HIGH FREQUENCY CROSS SECTIONS OF THE OCEAN SURFACE – COMPARISONS AND RECENT ENHANCEMENTS

Eric W. Gill[(1)] **John Walsh**[(2)]

[(1)]Faculty of Engineering and Applied Science, Memorial University of Newfoundland, St. John's, NF, A1B 3X5, Canada and E-mail:egill@engr.mun.ca

[(2)]As (1) above and also at Northern Radar Inc., P.O. Box 23039, St. John's, NF, A1B 4J9, Canada and E-mail:jwalsh@engr.mun.ca

ABSTRACT

Advancements in random rough surface scattering theory since the mid 1900's have led, in application, to the development of several high-frequency (HF)(3-30 MHz) radar cross section models for the ocean surface. Here, recent enhancements of these models are discussed. These involve (1) the proper use of the Pierson-Moskowitz nondirectional ocean spectrum in cross section modeling, (2) a correction to the high-Doppler cross section tails when radiation is scattered near the transmitting or receiving antennas and (3) an extension to the case of bistatic operation of pulsed Doppler surface wave radar.

INTRODUCTION

Over three decades, high frequency (HF) radar cross section models of the ocean surface have emerged to provide a two-fold utility: (1) the second-order model inversions lead to the determination of such oceanic parameters as significant waveheight, mean wave direction, and surface wind speeds, while first-order effects yield valuable information about surface currents and (2) the model characteristics give insight as to how to suppress ocean clutter when the radar is used in detecting and tracking ocean-going targets such as ships, icebergs and low-flying aircraft. These models have relied largely on scattering theory initiated by such investigators as Rice [1] and Walsh [2, 3, 4, 5].

All of the HF cross section models have been derived by assuming that surface deviations from the mean value are small compared to the radar wavelength and that the surface slopes are much less than unity. The first and perhaps best-known models resulted from extensive and excellent work by Barrick [6] based on Rice's perturbation analysis [1]. Next, Johnstone [7] presented another perturbation result but, as pointed out by Srivastava [8], it was erroneous in its statistical averaging associated with the electromagnetic and hydrodynamic effects. Because Srivastava's first- and second-order monostatic cross sections derived on the basis of [2] incorporate a pulsed dipole source, it differs from Barrick's in two major respects: (1) the first-order is a continuum rather than a weighted delta function and (2) the second-order contains an off-patch component as well as a contribution arising from scatter near the transmitting antenna.

The enhancements discussed here are based on the scattering theory found in [3, 4, 5]. These enhancements are three-fold and have been alluded to without elaboration by Gill and Walsh [9]. Firstly, the proper use in simulations of such ocean models as the Pierson-Moskowitz non-directional spectrum is considered. Secondly, it is shown that Srivastava's model for scatter at the transmitter is deficient in the form of its coupling coefficient. This problem results in Doppler spectral tails which are several dB too high. The new models are seen to follow physical reality much more closely. Thirdly, none of the previous models has extended the bistatic case to second order. While the latter has been presented by Gill and Walsh [9, 10], for completeness these more general expressions are repeated here with the corrections alluded to above.

CROSS SECTION ENHANCEMENTS

The Pierson-Moskowitz Spectrum in Cross Section Modeling

In the high frequency cross sections of the ocean surface presented in [9], the first order portion ${}_1\xi(x,y,t)$ of the scattering surface, where x, y and t are the usual spatial and temporal variables, is characterized as

$$ {}_1\xi(x,y,t) = \sum_{\vec{K},\omega} {}_1P_{\vec{K},\omega} e^{j\vec{K}\cdot\vec{\rho}} e^{j\omega t} \tag{1} $$

Here $\vec{K}(= K_x\hat{x} + K_y\hat{y})$ and ω are wavenumber and angular frequency, respectively, of the surface features and $\vec{\rho} = x\hat{x} + y\hat{y}$. The random roughness of the surface is established by taking the ${}_1P_{\vec{K},\omega}$ to be zero-mean Gaussian random variables. For a real surface, it may be further verified that

$$ {}_1P_{\vec{K},\omega} = \frac{1}{2}\left[P_{\vec{K}}e^{j\epsilon(\vec{K})}\delta_K\left(\omega+\sqrt{gK}\right)+P_{-\vec{K}}e^{-j\epsilon(-\vec{K})}\delta_K\left(\omega-\sqrt{gK}\right)\right] \tag{2} $$

with $P_{\vec{K}} = P^*_{\vec{K}}$ where $*$ denotes the complex conjugate (i.e. $P_{\vec{K}}$ is real), $\epsilon(\vec{K})$ is a random phase term, g is gravitational acceleration, and $\delta_K(\cdot)$ is the Kronecker delta. By allowing the fundamental spatial period of the surface to approach infinity, it is shown in [11] that the Fourier coefficients become

$$ P_{\vec{K}} = \sqrt{S_1(K_xK_y)dK_xdK_y} \tag{3} $$

it being understood that $S_1(K_x,K_y)$ is the first-order surface spectrum. On changing to polar coordinates and invoking the first order dispersion relationship for water waves, it may be deduced that

$$ {}_1\xi(x,y,t) = \int_0^\infty\int_{-\pi}^{\pi}\cos\left[(\omega^2/g)\left(x\cos\theta+y\sin\theta\right)-\omega t+\epsilon(\omega,\theta)\right]\cdot\left[2K(K/g)^{1/2}S_1(K_x,K_y)d\omega d\theta\right]^{1/2} . \tag{4} $$

Pierson's model [12] of a stationary Gaussian process, written in the notation of [9, 11], is

$$ {}_1\xi(x,y,t) = \int_0^\infty\int_{-\pi}^{\pi}\cos\left[(\omega^2/g)(x\cos\theta+y\sin\theta)-\omega t+\epsilon(\omega,\theta)\right]\left[S'_{PM}(\omega,\theta)d\omega d\theta\right]^{1/2} , \tag{5} $$

$S'_{PM}(\omega,\theta)$ being spectral density. Clearly, (4) and (5) agree if $S_1(K_x,K_y) = 0.5(g/K^3)^{1/2}S'_{PM}(\omega,\theta)$ or from (3)

$$ P_{\vec{K}} = \left[(1/2)(g/K^3)^{1/2}S'_{PM}(\omega,\theta)dK_xdK_y\right]^{1/2} . \tag{6} $$

Using (2) and (6) and carrying out the ensemble average $< {}_1P_{\vec{K},\omega}{}_1P^*_{\vec{K}',\omega'} >$ while noting that this correlation is also given in differential form by $S_1(K_x,K_y)dK_xdK_yd\omega$ and $S'_{PM}(\omega,\theta) = S_{PM}(K,\theta)\frac{dK}{d\omega}$, it may be deduced that

$$ \frac{1}{2}\sum_{m=\pm1}S_1(m\vec{K})\delta\left(\omega+m\sqrt{gK}\right)d\omega = \frac{1}{4}\left[\sum_{m=\pm1}S_{PM}(m\vec{K})\delta_K\left(\omega+m\sqrt{gK}\right)\right] . \tag{7} $$

Here, δ is the usual Dirac delta function while δ_K is the Kronecker delta, the two being related by $\delta\left(\omega+m\sqrt{gK}\right)d\omega = \delta_K\left(\omega+m\sqrt{gK}\right)$. $S_{PM}(\vec{K})$ is the usual Pierson-Moskowitz spectrum. Thus, it may be concluded that

$$ S_1(m\vec{K}) = \frac{1}{2}S_{PM}(m\vec{K}) . \tag{8} $$

Since the general spectra, represented by S_1, appearing in the cross sections of [9] are determined from ensemble averaging, then (8) indicates that the corresponding form of the Pierson-Moskowitz spectrum must be multiplied by a factor of 1/2 when replacing S_1 for modeling purposes.

A Correction to the Theory for Scatter at the Transmitting Antenna

Srivastava [8] developed a monostatic result for the second-order HF Doppler cross section component, corresponding to σ_{2T} of [9], involving a single scatter at the transmitter followed by another on a distant surface patch before reception. However, the high-Doppler tails of Srivastava's model are very flat beyond the $\pm2\omega_B$ singularities, ω_B being the Doppler positions of the Bragg frequencies (see Figure 1). While in [9] σ_{2T} is seen to enhance the overall second-order result beyond that of the patch scatter cross section, the fall-off of the tails is much more rapid than in Srivastava's presentation. This difference is addressed here and may be attributed to the forms of the electromagnetic coupling coefficient.

Using the notation of [9], the magnitude square of Srivastava's coupling coefficient, Γ_S, for what corresponds to the σ_{2T} cross section component, when the transmit wavenumber is k_0 may be written as

$$ |\Gamma_S|^2 = \frac{\left[2k_0\cos(\theta_{\vec{K}_2}-\theta_{\vec{K}_1})+2K_1)\right]^2}{\left|\frac{2k_0\cos(\theta_{\vec{K}_2}-\theta_{\vec{K}_1})}{K_1}+1\right|} . \tag{9} $$

Here the $\vec{K}_1$ and $\vec{K}_2$ are wavevectors of the scattering surface which give rise to σ_{2T}, and $\theta_{\vec{K}_1}$ and $\theta_{\vec{K}_2}$ are their respective

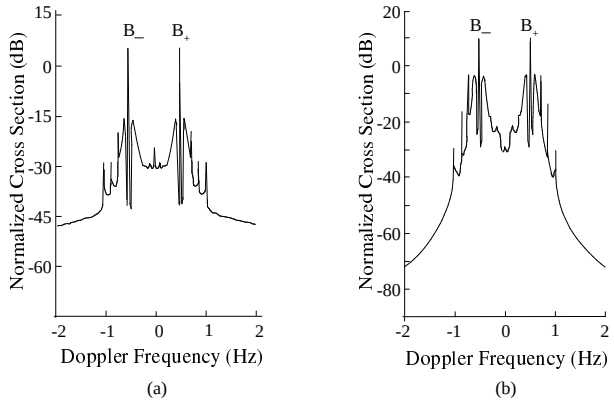

Figure 1: (a) Srivastava's cross section and (b) Gill's cross section for a 15 m/s wind 90° to beam and operating frequency of approximately 25 MHz. Monostatic operation is assumed. B_- and B_+ are the Bragg peaks.

directions. For the case of backscatter, it is noted that $\left|\vec{K}_2\right| = K_2 = 2k_0$, while K_1 increases as the magnitude of the angular Doppler frequency ω_d similarly increases. It is easily seen that as K_1 becomes large

$$|\Gamma_S|^2 \longrightarrow \left[2k_0 \cos(\theta_{\vec{K}_2} - \theta_{\vec{K}_1}) + 2K_1\right]^2 . \tag{10}$$

That is, for large K_1 or, equivalently, large $|\omega_d|$ the coupling coefficient similarly increases. The effect of this ever-increasing factor for large $|\omega_d|$ is mitigated by the reducing ocean spectrum, $S_1(\vec{K}_1)$, and the overall effect is to produce spectral tails which fall off more slowly than actual radar spectra would indicate.

From [9, 10], the quantity analogous to Γ_S is ${}_E\Gamma_T$ and it is straightforward to verify that for monostatic operation

$$|{}_E\Gamma_T|^2 = \frac{k_0^2\left[1 + \frac{k_0}{K_1}\cos(\theta_{\vec{K}_2} - \theta_{\vec{K}_1})\right]^2}{\left\{\left[1 + \frac{2k_0\cos(\theta_{\vec{K}_2} - \theta_{\vec{K}_1})}{K_1}\right]\left[1 + \frac{2k_0\cos(\theta_{\vec{K}_2} - \theta_{\vec{K}_1})}{K_1} - 2k_0\sqrt{\left|\frac{1}{K_1^2} + \frac{2k_0\cos(\theta_{\vec{K}_2} - \theta_{\vec{K}_1})}{K_1^3}\right|} - \left(\frac{k_0}{K_1}\right)^2\right]\right\}} . \tag{11}$$

In this form, it may be readily observed that as K_1 becomes unbounded

$$|{}_E\Gamma_T|^2 \longrightarrow k_0^2 . \tag{12}$$

Thus, as K_1, and consequently ω_d, increases, $|{}_E\Gamma_T|^2$ has an upper limit unlike Srivastava's coefficient. The ocean spectrum is, as before, decreasing rapidly so that the combined effect is that the high-Doppler tails of $\sigma_{2T}(\omega_d)$ should essentially follow that of the $S_1(K_1)$. This concludes the explanation of the difference between $\sigma_{2T}(\omega_d)$ and Srivastava's corresponding monostatic model.

BISTATIC CROSS SECTIONS

To second order in scatter, the bistatic cross section of the ocean using a HF surface wave Doppler radar may be summarized as

$$\sigma(\omega_d) = \sigma_{11}(\omega_d) + \sigma_{2P}(\omega_d) + \sigma_{2T}(\omega_d) + \sigma_{2R}(\omega_d) \tag{13}$$

where the first term represents the contribution from a single scatter (i.e a first-order result) and the last three terms arise from double scattering as follows: σ_{2P} is due to two scatters on a patch of ocean remote from the radar components – it also includes a single scatter from second-order ocean waves; σ_{2T} is from a scatter near the transmitter followed by another on the remote patch; and σ_{2R} is from a scatter near the receiver following a previous scatter on the remote patch. The first-order term normalized to the patch area is given by

$$\sigma_{11}(\omega_d) = 2^4\pi k_0^2 \Delta\rho_s \sum_{m=\pm 1} S_1(m\vec{K})\frac{K^{\frac{5}{2}}\cos\phi_0}{\sqrt{g}}\mathrm{Sa}^2\left[\frac{\Delta\rho_s}{2}\left(\frac{K}{\cos\phi_0} - 2k_0\right)\right] . \tag{14}$$

Here, $\Delta\rho_s$ is the patch width, Sa[ ] is the sampling function and ϕ_0 is the bistatic angle. It should be observed, for the purpose of distinguishing $\sigma_{11}(\omega_d)$ from the higher-order cross section components, that $\vec{K}$ is associated with a first-order

ocean wave. The second-order "patch scatter" cross section is given as

$$\sigma_{2P}(\omega_d) = 2^3\pi k_0^2 \Delta\rho_s \sum_{m_1=\pm1}\sum_{m_2=\pm1}\int_0^\infty\int_{-\pi}^{\pi}\int_0^\infty \left\{S_1(m_1\vec{K}_1)S_1(m_2\vec{K}_2)\left|{}_s\Gamma_P\right|^2 K^2\cos\phi_0 \cdot \mathrm{Sa}^2\left[\frac{\Delta\rho_s}{2}\left(\frac{K}{\cos\phi_0}-2k_0\right)\right]\delta\left(\omega_d + m_1\sqrt{gK_1}+m_2\sqrt{gK_2}\right)K_1\right\} dK_1 d\theta_{\vec{K}_1} dK \ . \quad (15)$$

Here, $\vec{K}_1$ and $\vec{K}_2$ are the wave vectors of first-order ocean waves while $\vec{K}$ is their sum (i.e. $\vec{K}_2 = \vec{K} - \vec{K}_1$). Also, δ is the Dirac delta function and ${}_s\Gamma_P$ is a symmetricized form of the patch scatter coupling coefficient described in [9, 10]. The term σ_{2T} has the same form as (15) but with 2^3, K and ${}_s\Gamma_P$ replaced by 2^2, $K_2(\approx 2k_0\cos_{\phi_0})$ and ${}_E\Gamma_T$, respectively. For σ_{2R}, the corresponding replacements are 2^2, $K_1(\approx 2k_0\cos\phi_0)$ and ${}_E\Gamma_R$, respectively, the latter being another coupling coefficient found in [9, 10]. It may be noted that the presence of $\mathrm{Sa}^2[\ ]$ ensures that, unlike some previous models, even the first-order result is a continuum.

SUMMARY

New initiatives regarding the high frequency pulse radar cross sections of the ocean surface have been considered. It has been concluded that, for inclusion in cross section modeling, ocean spectra of the Pierson-Moskowitz type should be multiplied by a factor of 0.5. Furthermore, corrections to the high-Doppler tails found in [8] have been presented and illustrated in the context of new HF bistatic ocean surface cross sections. It is hoped that continuing enhancements to these models will provide further improvements to their use in ocean parameter measurement and a better understanding of the fundamental mechanisms involved in the scattering of electromagnetic radiation from random, time-varying surfaces.

REFERENCES

[1] S. Rice, "Reflection of electromagnetic waves from a slightly rough surface," in *Theory of Electromagnetic Waves* (K. Kline, ed.), pp. 351–378, New York: Interscience, 1951.

[2] J. Walsh, "On the theory of electromagnetic propagation across a rough surface and calculations in the VHF region," OEIC Report N00232, Memorial University of Newfoundland, St. John's, Newfoundland, 1980.

[3] J. Walsh and R. Donnelly, "A new technique for studying propagation and scattering for mixed paths with discontinuities," *Proc. R. Soc. Lond. A 412*, pp. 125–167, 1987.

[4] J. Walsh and R. Donnelly, "A consolidated approach to two-body electromagnetic scattering problems," *Phys. Review A*, vol. 36, no. 9, pp. 4474–4485, 1987.

[5] J. Walsh and S. Srivastava, "Rough surface propagation and scatter 1. General formulation and solution for periodic surfaces," *Radio Science*, vol. 22, no. 2, pp. 193–208, 1987.

[6] D. Barrick, "Remote sensing of sea state by radar," in *Remote Sensing of the Troposphere* (V. Derr, ed.), ch. 12, pp. 1–46, Washington, DC: U.S. Government Printing Office, 1972.

[7] D. Johnstone, "Second-order electromagnetic and hydrodynamic effects in high-frequency radio wave scattering from the sea," Technical Report 3615-3, Stanford Electronics Laboratories, Stanford University, California, 1975.

[8] S. Srivastava, *Analysis of HF scattering from an ocean surface: An alternative approach incorporating a dipole source*. PhD thesis, Memorial University of Newfoundland, St. John's, Newfoundland, 1984.

[9] E. Gill and J. Walsh, "High-frequency bistatic cross sections of the ocean surface," *Radio Science*, vol. 36, no. 06, pp. 1459–1475, 2001.

[10] E. Gill and J. Walsh, "The bistatic form of the electric field equations for the scattering of vertically polarized high frequency ground wave radiation from slightly rough, good conducting surfaces," *Radio Science*, vol. 35, no. 06, pp. 1337–1359, 2000.

[11] E. Gill, *The Scattering of High Frequency Electromagnetic Radiation from the Ocean Surface: An Analysis Based on a Bistatic Ground Wave Radar Configuration*. PhD thesis, Memorial University of Newfoundland, St. John's, Newfoundland, 1999.

[12] W. Pierson, "Wind generated gravity waves," *Advances in Geophysics*, vol. 2, pp. 93–178, 1955.